# On the cleansing and inspection of GPS ephemeris data 2000–2016

Arne Lie, Aiden Morrison, and Nadezda Sokolova
SINTEF Digital
Trondheim, Norway
Email: arne.lie, aiden.morrison, nadia.sokolova@sintef.no

Morten Topland
Indra Navia AS
Oslo, Norway
Email: morten.topland@indra.no

***Abstract*—Archived GPS ephemeris data for years 2000-2016 is investigated by cleansing and precision measures. The goal of this work was twofold: (1) to reveal and remove incorrect ephemeris data so that the cleansed data is as close to the real broadcasted data as possible, and (2) to analyse the quality of the cleansed data by comparing ephemeris based satellite locations to true locations. Our findings show that, besides obvious duplicates, many erroneous data epochs were also detected by monitoring the slowly changing $I_0$ and $\Omega_0$ parameters. The cleansed data shows small deviation precision errors steadily decay in the 2000–2016 period, as expected. Also the number of large errors show a decaying nature. Many large errors occur frequently in first operation period of new satellite vehicles, especially the new Block IIF, but these happened also to show in time epochs close to periods flagged as unhealthy. Further, it is shown that ephemeris data performance is independent on $T_{oe}$ parameter being modulo 100 or not.**

***Keywords*—GPS; satellite; navigation; ephemeris**

## I. Introduction

Ephemeris data is key to nearly all GNSS location services, and while this study was performed in the context of Ground Based Augmentation System (GBAS) development, it is of potentially greater interest to single-point positioning users as these lack the benefit of a stationary reference receiver with which to detect and exclude ephemeris anomalies. The 15 parameters that constitutes the GPS ephemeris provide an expanded Keplerian data set for (precise) nominal satellite orbit description, valid for a 2-4 hour time window. Every two hours, a new set of ephemeris data is broadcast from each of the (up to) 32 orbiting satellites. The five main control segment ground stations are responsible for forecasting and calculation of new ephemeris data sets and uploading these to the space segment. A GPS user receiver must decode the ephemeris and calculate the pseudorange from at least four satellites to be able to calculate its own position, while the calculated position accuracy is dependent on the quality of the ephemeris data among other parameters.

If a monitoring ground station detects large deviations between the controlled satellite position and its ephemeris data, it will set the health status of the satellite to unhealthy. GPS receivers disregard signals from unhealthy vehicles, and will select signals from healthy vehicles only. To assist GPS network operation performance validation, the tracked (true) satellite orbit positions are logged into open databases, e.g., the ftp site cddis.gsfc.nasa.gov in the sp3 format, (which provides the final or precise orbits used in this paper). Additionally, the broadcast ephemeris from all orbiting satellites are logged by the CORS (Continuously Operating Reference Station) network, and a comprehensive global set can be downloaded from ftp://geodesy.noaa.gov/cors/rinex (the `brdc*.*n` files).

The latter GNSS ephemeris data needs cleansing, before it can be confidently stated that they represent the ephemeris data actually broadcast by the satellites. Some of the factors which cause incorrect ephemeris data to be stored in these repositories include firmware errors in the receivers used in the collection system, erroneous transmission, as well as other unlikely but possible sources.

Once cleansed, one can obtain insight into the quality of the retrieved ephemeris, by comparing the position difference between ephemeris based and reference sp3 based satellite positions at each epoch. The contribution of this paper is a comprehensive analysis of archived data from the years 2000-2016, to reveal large and small anomalies in the broadcasted ephemeris, where the processing includes both cleansing followed by GPS vehicle position accuracy validation. Related works include Warren [1] and Heng et al. [2], [3], where similar cleansing methods have been applied, but where performance accuracy is measured using the much more CPU demanding geometric-analytic worst-case SISRE vs. $4.42 \times URA$ [1] upper bound approach. In contrast, we calculate the satellite position error vector magnitude and compare it to a fixed threshold and a dynamic threshold based on broadcasted URA values. Further the results are sorted per SVN (Satellite Vehicle Number) identity, as well as vs. time, to provide insight into how position accuracy varies per satellite blocks and with satellite age. To the best of our knowledge this is the first publication that covers GPS position accuracy statistics sorted by these metrics.

## II. Background and motivation

While the likelihood that erroneous ephemeris terms will cause an unacceptably large satellite apparent position error depends on the likelihood of detection and exclusion of such errors, the severity of the impact of this failure mode also depends on the way in which the received signals are utilized. In the case of the GBAS, GNSS signals are received by an array of up to four ground based receivers which are responsible for the calculation of reliable correction terms, and their transmission to airborne users at short latency. Since the GBAS system has very demanding availability and continuity requirements it is necessary that monitors which check for failure modes such as erroneous ephemeris will have a low

false alarm rate, as well as a short initialization time and a rapid reaction time. Since safety of life depends on the integrity of the service, it is also essential that the monitors have an extremely low rate of missed detection. Even though the common mode line of sight errors between the relatively close ($< 6$ km) aircraft and the ground based receivers cancels out, the accuracy requirements of the GBAS system dictate a low tolerable limit on residual errors. Because the calculated satellite position errors introduced by an ephemeris fault can produce an apparent satellite position error ranging from very small to very large it is not possible to make a prior assumption about the likely magnitude of such errors. Thus, ephemeris position error statistics are useful with respect to deriving GBAS integrity monitor performance with respect to false alarms. Similarly, any application whether single point or differential can benefit from an understanding of these same statistics.

## III. Cleansing Methodology

### A. Background and cleansing methods used

The supported ephemeris cleansing method from the literature [2], from which our method takes inspiration, includes basically two stages: sorting and inconsistency checking. Our sorting method performs, for each day of investigation:

- Correct the reference time by ensuring consistent wraparound when week changes.
- Remove data entries that do not belong to the current day.
- Find entries from the previous and next day that belong to the current day.
- Add these entries to the current day.

The ephemeris data sets typically holds duplicates, especially at epochs close to midnight. Our findings show that such duplicates are more frequent in years 2008–2016 than in 2000–2007.

These sorted data are then fed into our second cleansing stage, the inconsistency check. Here, the objective is to identify ephemeris sets that hold obvious errors that make them highly unlikely to have ever been broadcast. Three metrics used to check for this condition are

1) the $T_{oe}$ parameter (reference time of ephemeris) is required to have 00 as least significant digits, and
2) right ascension $\Omega_0$ and inclination angle $I_0$ parameters should change slowly per satellite in time.
3) Duplicates identified as ephemeris data only 16 s or less apart: remove one.

The first metric was inspired by earlier investigations that did find instances of bad ephemeris data having non-00 ending $T_{oe}$. When it comes to metric two, single outliers can be easily detected by comparing values to neighbour values within 6 hour time window. In addition, selected parameters are inspected for obvious errors, such as $\sqrt{A} = 0$ ($A$: semi-major axis). The resulting data is shown in Table I.

A full set of ephemeris per non-leap year for a 32 satellite constellation comes to $32 \times 12 \times 365 = 140160$ ephemeris

Table I. Cleansing results from our initial work

| Year | Tot. Eph data | Removed by sorting | Duplicates | Inconsistent & non-00 Toe | Cleansed |
|---|---|---|---|---|---|
| **2000** | 129443 | 1 | 9305 | 11968 | 108169 |
| **2001** | 139819 | 1241 | 13796 | 14930 | 109852 |
| **2002** | 133286 | 694 | 10913 | 13506 | 108173 |
| **2003** | 134537 | 1 | 11401 | 13672 | 109463 |
| **2004** | 136896 | 82 | 11310 | 13122 | 112382 |
| **2005** | 138702 | 0 | 11546 | 12871 | 114285 |
| **2006** | 138301 | 0 | 10874 | 12349 | 115078 |
| **2007** | 146613 | 0 | 11483 | 13382 | 121748 |
| **2008** | 158957 | 5612 | 17050 | 14435 | 121860 |
| **2009** | 166992 | 7110 | 21018 | 13843 | 125021 |
| **2010** | 172313 | 11341 | 21180 | 13925 | 125867 |
| **2011** | 176450 | 16018 | 22187 | 12715 | 125530 |
| **2012** | 180500 | 20315 | 22247 | 13059 | 124879 |
| **2013** | 174600 | 21130 | 14996 | 12659 | 125815 |
| **2014** | 165582 | 10208 | 17829 | 12950 | 124595 |
| **2015** | 167725 | 10474 | 18794 | 12966 | 125491 |

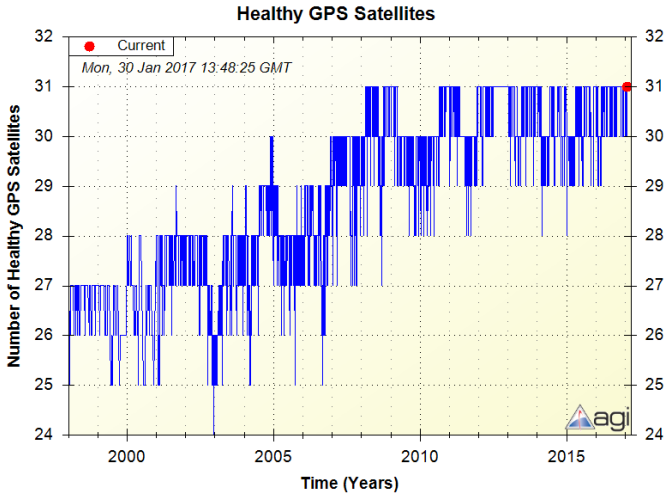


Figure 1. Number of healthy satellites copied from [4]

sets. Available data for healthy satellites says that the number is smaller: from about 27 satellites in year 2000 there is a fairly linear increase towards 31 satellites in 2008, and since then 30–31 satellites have been generally healthy, see Fig. 1. So, 118000–135000 ephemeris data should be expected. The cleansing algorithm described above results in approximately only 108000–125000 ephemeris sets (see rightmost column in Table I), implying that also perfectly good data is being removed.

### B. Cleansing algorithm refinements

It was discovered after some further investigation that the general assumption of data having two last digits in $T_{oe}$ not equal 00 was implicitly bad data, actually did not hold up. For some of the investigated years such data was also frequent, and when simply removed, the leftover ephemeris data for some PRNs could become so sparse that the inconsistency check algorithm became consequently unfit to remove bad data. In addition it was discovered that some data had a mismatch between its $T_{oe}$ value and the time–stamp $t_{eph}$ given

Table II. CLEANSING RESULTS USING REVISED METHOD

| Year | Removed by "Toe offset" | Tot. Eph data | Removed by sorting | Duplicates | of which caught in triplet filter | Inconsi-stent | Cleansed |
|---|---|---|---|---|---|---|---|
| 2000 | 406 | 129038 | 0 | 9475 | '8 / 3' | 13 | 119550 |
| 2001 | 32 | 139787 | 1229 | 15030 | '1051 / 0' | 17 | 123511 |
| 2002 | 22 | 133264 | 692 | 11054 | '2 / 0' | 35 | 121483 |
| 2003 | 22 | 134515 | 0 | 11598 | '0 / 0' | 6 | 122911 |
| 2004 | 261 | 136636 | 80 | 11394 | '6 / 0' | 6 | 125156 |
| 2005 | 13 | 138689 | 0 | 11683 | '0 / 0' | 23 | 126983 |
| 2006 | 0 | 138301 | 0 | 11028 | '0 / 0' | 17 | 127256 |
| 2007 | 0 | 146613 | 0 | 11625 | '0 / 0' | 187 | 134801 |
| 2008 | 0 | 158957 | 5612 | 17101 | '0 / 0' | 30 | 136214 |
| 2009 | 0 | 166992 | 7110 | 21018 | '0 / 0' | 140 | 138724 |
| 2010 | 0 | 172313 | 11341 | 21130 | '0 / 0' | 480 | 139362 |
| 2011 | 0 | 176450 | 16018 | 22186 | '0 / 0' | 86 | 138160 |
| 2012 | 0 | 180500 | 20315 | 22246 | '0 / 0' | 93 | 137846 |
| 2013 | 0 | 174600 | 21130 | 14997 | '0 / 0' | 59 | 138414 |
| 2014 | 0 | 165582 | 10208 | 17923 | '0 / 0' | 123 | 137328 |
| 2015 | 0 | 167725 | 10474 | 18796 | '0 / 0' | 54 | 138401 |
| 2016 | 0 | 162637 | 11265 | 10940 | '0 / 0' | 15 | 140417 |

to the header of the ephemeris log file. Such data having $|T_{oe} - t_{eph}| > 0$ ("$T_{oe}$-offset") produced some very large position deviations relative to true values, and thus could not be trusted. We modified our sorting algorithm accordingly:

1) Ephemeris data with "$T_{oe}$-offset" larger than 0 is removed.
2) The filter removing all data with non-00 ending $T_{oe}$ was modified to a "triplet equality filter", in that data removal only takes place if the slowly varying $I_0$ and $\Omega_0$ parameters, and the $M_0$ (mean anomaly reference) parameter, are all equal to at least one of the closest data neighbours in time.
3) Inconsistency check time window increased from 6 hour to cover whole day (24 hours), to better cope with sparse data.

The results (Table II) show that about 10 % more data survives the cleansing. Triplet-filter has identified erroneous non-00 ending $T_{oe}$ ephemeris data only in years 2000–2004, and the number of such occurrences is small (number before slash means a match is found looking back in time, and after slash means a match is found looking forward in time). This also reveals that the number of data removed due to the inconsistency check time window is limited. The "$T_{oe}$-offset" filter has also removed data only in the first years (2000–2005). The majority of data removed from the set are pure duplicates. The resulting number of data surviving the cleansing (right-most column) are now more inline with the expected number of ephemeris data (118000–135000). Still, note that the data sets can be sparse for some PRNs in some periods, while for others, more than 12 ephemeris data sets per day can have survived the cleansing.

## IV. ANALYSIS OF EPHEMERIS DATA QUALITY

### A. On PRN to SVN mapping

Each of the (up to 32) active satellites is uniquely identified by its PRN code (Pseudo Random Noise sequence, numbered 1–32), and this code is therefore also logged in the ephemeris data and true data repositories. The physical satellite vehicle that is actually using these PRNs is not logged. However, since this mapping has changed slowly over time, other sources can be found that hold this information, e.g., ftp://igs.org/pub/station/general/igs08.atx. Some PRN numbers have been hosted by only a small number of vehicles, while others such as PRN 30 has been hosted by 8 vehicles: SVN 30 starting September 1996, via SVN 35, 49, 32, 37, 27, 49, and finally SVN 64 starting February 2014. Over 70 GPS satellites have been launched in total, divided into multiple technology Blocks:

- Block I: SVN 1 was launched 22 February 1978 (Block I consists of SVN 1–11)
- Block II: SVN 14 launched 14 February 1989 (Block II consists of SVN 13–21)
- Block II-A: SVN 23 launched 26 November 1990 (Block II-A consists of SVN 22–40)
- Block II-R: SVN 42 launched 17 January 1997 (Block II-R consists of SVN 41–47, 51, 54, 56, and 59–61)
- Block IIR-M: SVN 53 launched 26 September 2005 (Block IIR-M consists of 48–50, 52–53, 55, and 57–58)
- Block IIF: SVN 62 launched 28 May 2010 (Block IIF consists of SVN 62–73, last launched is SVN 70 on 5 February 2016)

In the investigated time span 2000-2016 more than 20 new satellite launches have taken place. The last retired IIA vehicle (SVN 23) was kept in operation until January 25, 2016, after 26 years in service. Other IIA block satellites that were kept in service for extended time include SVN 30 (15 years, retired July 20 2011), SVN 33 (18 years by August 2, 2014), SVN 39 (21 years by May 19 2014), SVN 26 (23 years by January 6 2015), SVN 24 (20 years), SVN 25 (17 years). Eight other Block IIA vehicles are still kept in orbit as reserve (as of summer 2016), i.e., SVN 27, 32, 34, 35, 36, 37, 38, and 40.

In this paper we wanted to investigate if large errors were correlated to satellite age, or satellite Block generations, or even specific SVNs. We have therefore created data structures that map PRN to SVN numbers over time, using the information found in ftp://igs.org/pub/station/general/igs08.atx.

### B. Analysis methodology

The cleansed data was validated against "true" satellite data, acquired from SP3 files in ftp://cddis.gsfc.nasa.gov. The true data is presented as satellite vehicle positions every 15 minutes, i.e., $4 \times 24 = 96$ positions each day per satellite. Note however that this data set too can hold invalid or missing data. Such findings are counted as "defect comparison" in final summary Table III.

Instead of following the reference literature approach of comparing true positions to ephemeris based calculated positions every 15 minutes, we based our comparison on the ephemeris data file sets and used the $T_{oe}$ and PRN values to select the SP3 true data positions with time–stamp $t_{sp3}$ with least deviation from the ephemeris $T_{oe}$ (not more different than $\pm 1$ hour), and then calculate satellite vehicle position

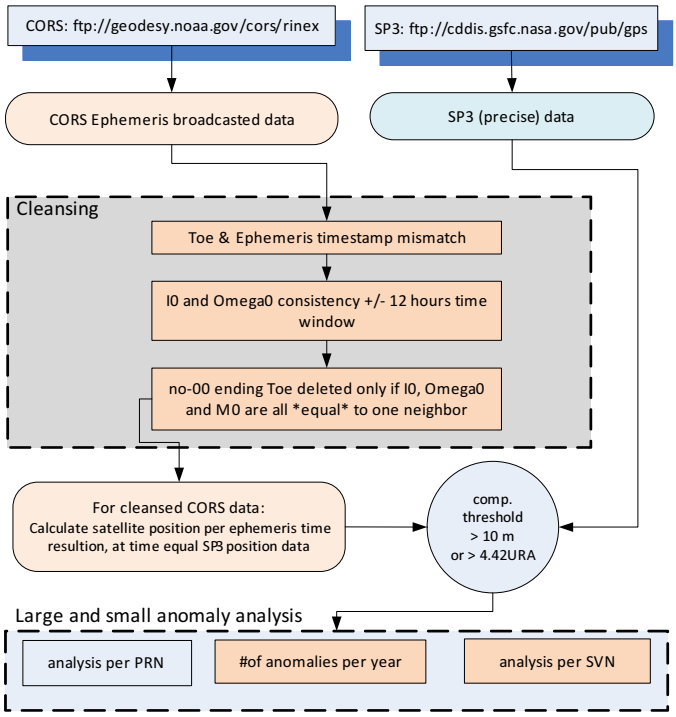


Figure 2. Cleansing the CORS ephemeris data comparison analysis to true satellite positions

at the time $t_k = t_{sp3} - T_{oe}$. On average this means 8 times less comparisons (one per two hours) without losing statistical confidence, since the validity of each ephemeris is 4 hours. In case the selected SP3 data turned out to be invalid, the comparison is skipped and flagged as "defect comparison", as noted above.

To simplify further, we have calculated the true ECEF distance offset regardless of error vector axial direction. The projection into precise earth surface user range accuracy is thus not calculated. The justification for this approximation is that our work has focussed on large errors and their frequency. The need for precise projection can therefore be relaxed.

Our Matlab®-based cleansing and analysis software structure is depicted in Fig. 2 where we have emphasized the modified cleansing functions and that we in the following will show results per year, and per SVN identity.

### C. Small errors

Despite of the absence of error vector precise surface projection we present the calculated small error mean and standard deviation, as well as look into how each SVN and block generation perform. Here, we have selected small error to be all error vectors of magnitude 50 meters and less. As we see from Fig. 3 there has been a linear decrease of the mean error (of all active SVNs) from about 4.5 m in year 2000 to about 1.5 m in 2008. Since that year, the mean has been steady at 1.5 m. Fig. 4 shows that error $< 0.5$ m has been almost absent for SVN 41–47 and 51, 54, and 56 (Block IIR), as well as all of the recently launched Block IIF. However, Fig. 5 shows that Block IIF mean error is small and Fig. 6 shows that its standard deviation has improved over the 6 years it has been operating.

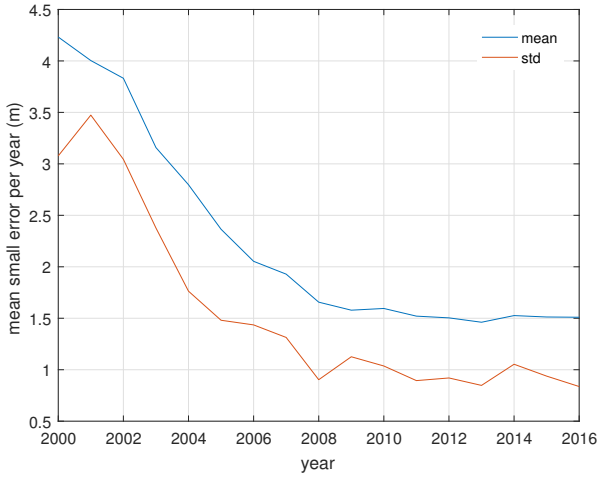


Figure 3. Errors $< 50$ m mean and standard variance per year of all healthy satellites

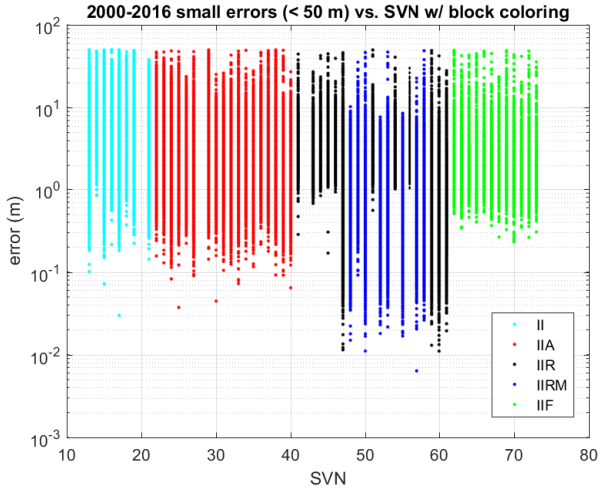


Figure 4. Small errors $< 50$ m vs. SVN

The latter figure also shows a peculiar Block IIR behavior in that its vehicles at age about 13 years has increased mean but decreased std. Actually, most of the SVNs shows decreased std, which is inline with the general findings. The reason for this different behavior of the block IIR-M satellites after a specific date is thought to be due to differences in control segment handling of clock error prediction for these satellites after this point, but no confirmation of this supposition has been found.

### D. Large errors

The ground segment has two main measures to activate when large deviations are detected: increase the broadcasted URA parameter value (User Range Accuracy), or signal this vehicle as unhealthy by setting Health bit to 1 (or 63). URA can be considered a soft measure that GPS receivers can utilize in order to weight the observation and predict the accuracy of its fixed position. While signals having large URA values can be rejected or de-weighted for fixing the position, signals flagged as unhealthy should be completely avoided. URA is

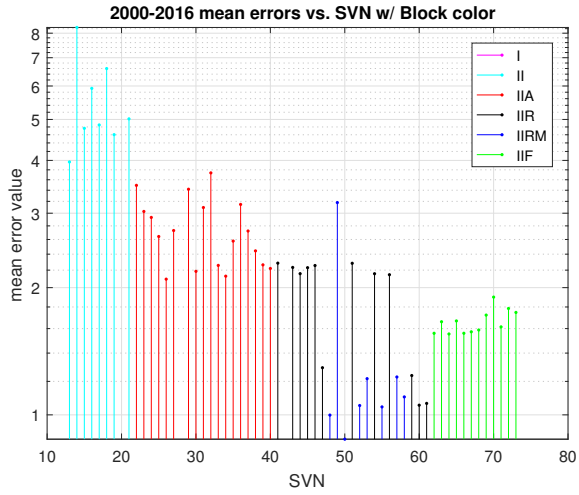


Figure 5. Small errors ($< 50$ m) mean values vs. SVN

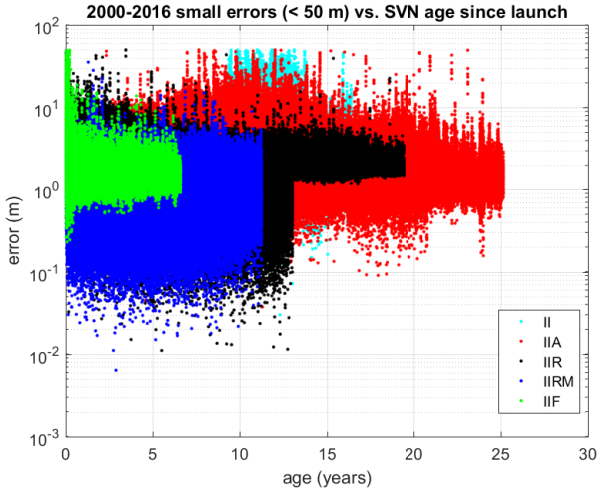


Figure 6. Small errors ($< 50$ m) vs. SVN age

a statistical indicator of the GPS ranging accuracy obtainable with a specific signal and SVN. URA provides a conservative RMS estimate of the user range error (URE) in the associated navigation data for the transmitting SVN. It includes all errors for which the Space and Control Segments are responsible. Whether the integrity status flag is 'off' or 'on', $4.42 \times URA_{ub}$ bounds the instantaneous URE under all conditions with $1 - 10^{-5}$ per hour probability.

In our work we have considered two different measures for detecting large errors:

1) error $> 4.42 \times URA_{ub}$ (m), and
2) error $> 10$ (m),

where $URA_{ub}$ denotes URA Upper Bound, which is tabulated in [5] page 88–89. In general, the former metric counts somewhat fewer errors than the latter.

In particular, we want to investigate the following questions:

$T_{oe}$ Are ephemeris data holding $Toe$ values with two least significant digits not ending on 00 of lesser quality?

Block Are some Blocks of satellites reasonably expected to have higher error probability than others?

Age Will old satellite vehicles have increased probability of large errors?

Healthy Is it likely that "healthy" ephemeris data will contain errors if earlier or later ephemeris close in time from same satellite have been flagged as unhealthy?

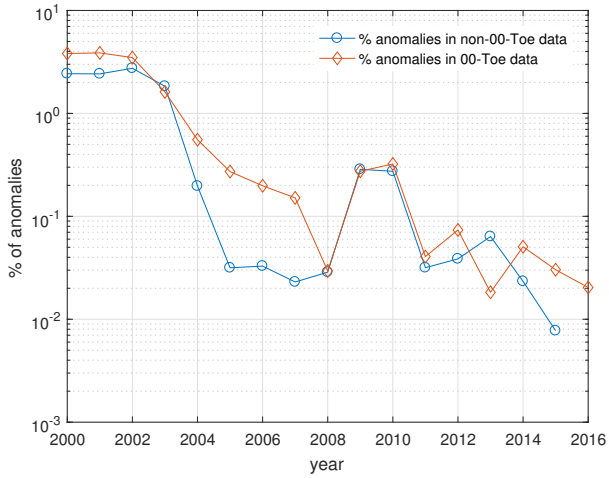


Figure 7. Large errors per year sorted depending on $T_{oe}$ value

*1) Non-00 ending $T_{oe}$:* We have used error criteria 2 and counted the percentage of all error data that are caused by Non-00 ending $T_{oe}$ and 00 ending $T_{oe}$ data. The results can be inspected in Fig. 7. Both curves have decaying error-count in the year span, and their magnitude is very nearly equal. The details reveal however that surprisingly, non-00 ending $T_{oe}$ data has lower error counts than the other group, for all years except 2013. The local peak of year 2009–2010 is due to a malfunctioning SVN-49 and will be discussed in next subsection.

*2) Block dependency:* We have used error criteria 2 and used all data irrespective of type of $T_{oe}$ value, and sorted the errors versus time, SVN block and SVN age. Note that though Block I is depicted in some figures, there are no Block I satellites actively involved in the 2000–2016 data, and this block should therefore be disregarded.

Fig. 8 reveals when each error has taken place (time along y-axis, format "yy.mm.dd"), versus SVN associated with the ephemeris. This figure also tells us that the last of the Block II vehicles ceased operation in 2007, as well as the subsequent arrival of Block IIR-M and IIF satellites. We have already mentioned Block IIR-M being initially launched in 2005, so the figure also tells that large errors did not appear before 4 years after launch. In this plot the dominant IIR-M error source is SVN 49 (longer blue line in the middle of the figure), a vehicle launched 24 March 2009 with an experimental test payload for L5 transmission which caused signal degradation for L1/L2 users and therefore never entered active service [6], [7]. Somehow, the archived ephemeris files

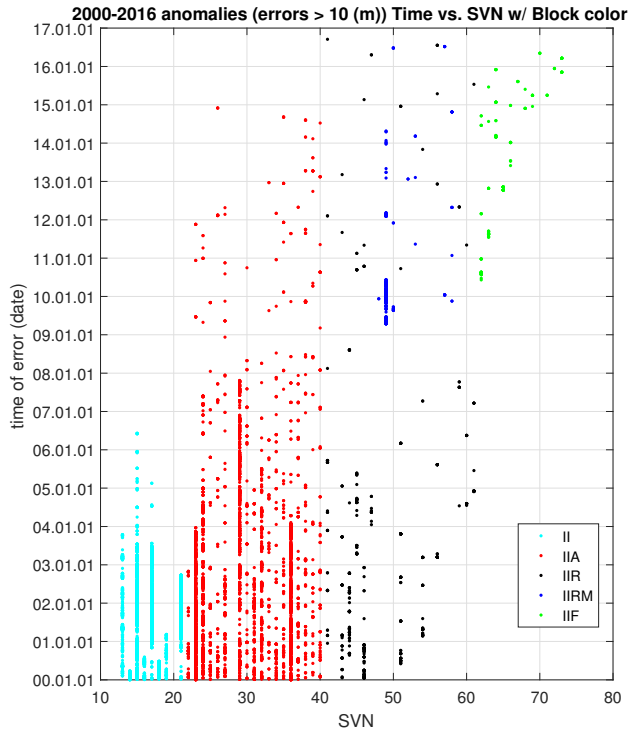


Figure 8. Large errors epochs vs. SVN

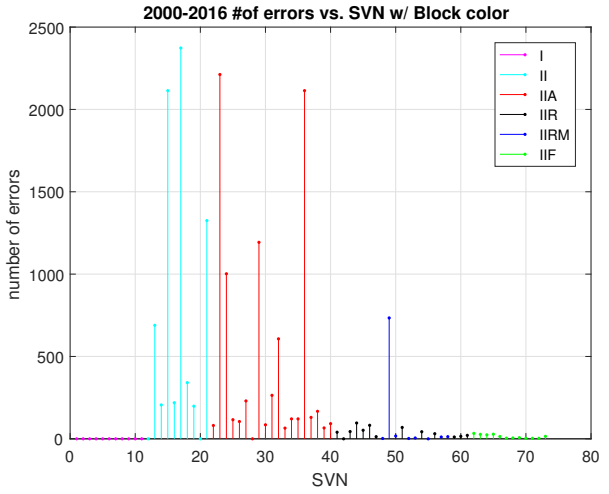


Figure 9. Number of large errors vs. SVN

occasionally report the health-flag set OK for this vehicle. We have in the following subsections kept SVN-49 in the data set, but special treatment is provided in the final investigations to highlight and/or exclude these "known bad" ephemeris sets from the analysis.

In Fig. 9 the number of large errors are depicted per satellite. It is obvious that Block II vehicles has highest number of errors, followed by Block IIA, and naturally fewest on the youngest generations. SVN 49 can be clearly spotted, as well as Block IIA SVN 23 and 36. The size of these errors

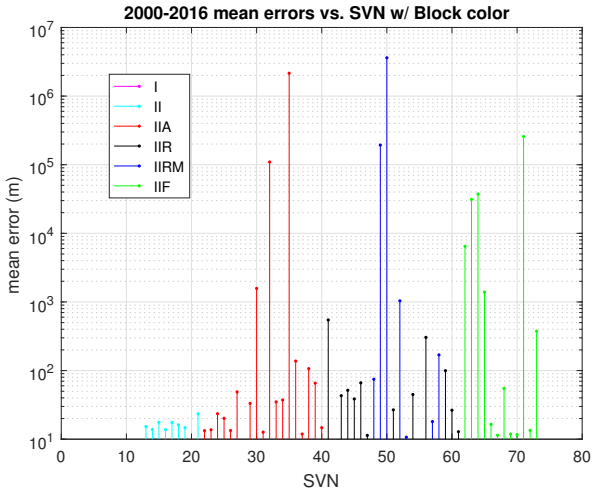


Figure 10. Mean of large errors sizes vs. SVN

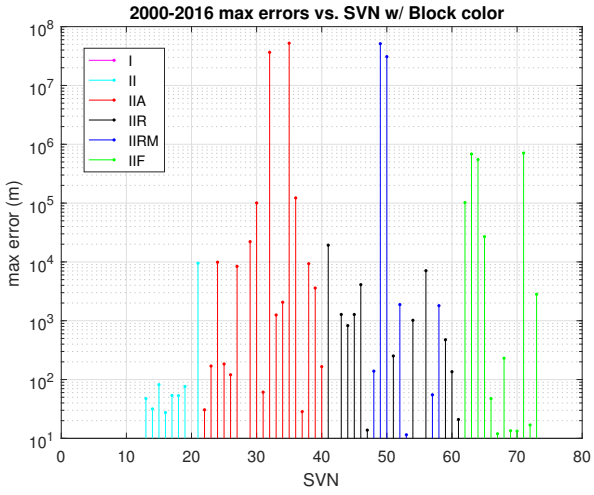


Figure 11. Maximum of large errors sizes vs. SVN

are not necessarily correlated with the number of errors, as revealed in Fig. 10 and 11, showing mean and maximum errors, respectively, per SVN. Here, SVN 32, 35, 49, 50, 63, 64, and 71, have higher values compares to the rest. Lastly, Fig. 12 depicts all error event as magnitude vs. SVN number.

*3) Age dependency:* In Fig. 13 we have displayed all error events with magnitude along y-axis and age of the causing SVN along x-axis. From this figure we can read: Block IIF satellites have been subject to large errors in its very first period of operation (green dots), and some very large errors also occur for Block IIR-M (blue dots) at about 1 and 4 year age. Block IIR-M vehicles also has had a "sticking" or persistent error of about 150 meters in first phase of operation (which turns out to be the faulty SVN 49). Block IIA (red dots) satellites have increasing error std towards about 10 years after launch, and then a decay after 10 years, while Block II (cyan dots) had a larger std than new newer Block IIA, but much fewer very large errors. There are a few very large Block IIA errors starting from the age range 14–20, which supports ageing SVN

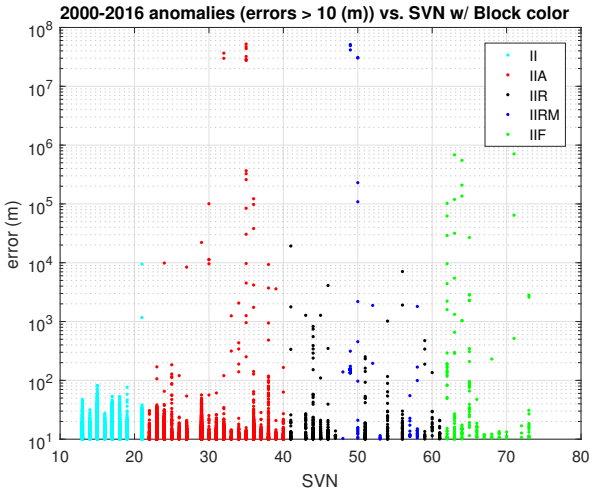


Figure 12. Large error magnitude vs. SVN, sorted into block generation

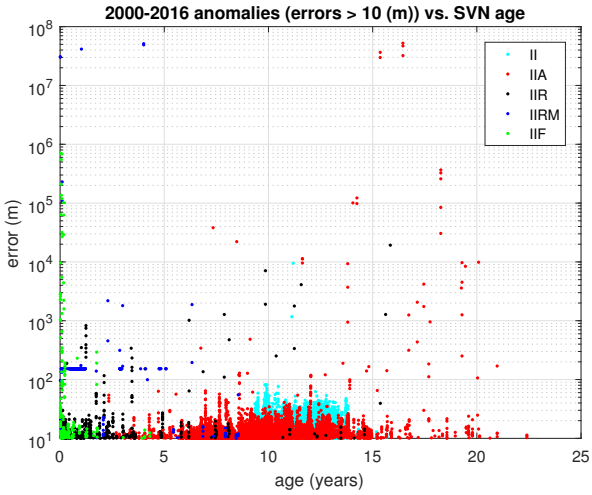


Figure 13. Large errors vs. SVN age, sorted into block generation

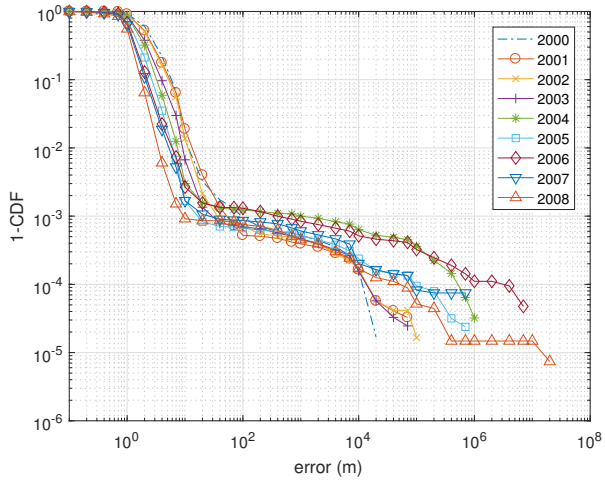


Figure 14. 2000–2008 all errors plotted as $1 - CDF$

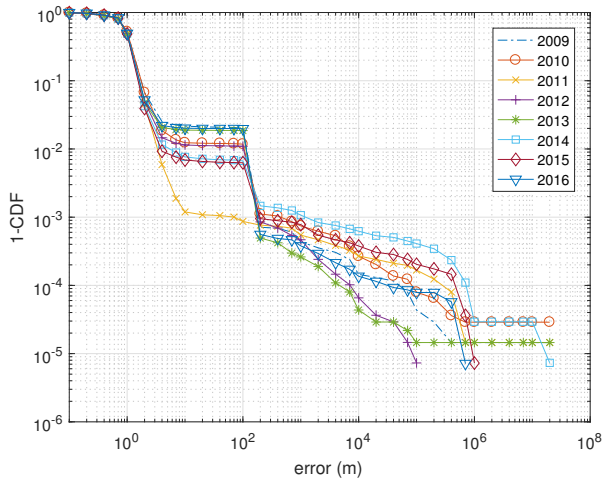


Figure 15. 2009–2016 all errors plotted as $1 - CDF$

vs. error correlation hypothesis somewhat.

*4) Health flag dependency:* The last issue we wanted to investigate was if large errors (again, only error criteria 2 is used) correlates with time epochs where the same satellite has an unhealthy status in an adjacent time period. For simplicity, we have selected same day as time window for searching such unhealthy status, irrespective of the exact time of day the large error occurs. The following figures have filtered out large errors if "all-day healthy" is marked in the figure caption. The following four figures shows $1 - CDF$ (cumulative density functions) of the error sizes across all active SVNs, divided into years. To increase readability, we have divided the figures into year 2000–2008 and 2009–2016, to be able to spot each year more easily. Fig. 14 and 15 show all errors irrespective of unhealthy ephemeris transmissions the same day. In the first figure we can read that errors of size 10–100 meters accounts for about 99 % of the data, with an increasing percentage at increasing year count, which tells that medium sized errors have been reduced in the years 2000–2008. For 0.1 % or less of the data there are error events of size 100 m and up to $10^7$ m. In Fig. 15 we see that the medium sized errors are constant, but there are errors events of size 100–200 meters that creates the "jump" in the curve. SVN 49 is one clear contributor here.

In Fig. 16 and 17, all errors belonging to days where the same satellite has signalled unhealthy ephemeris data have been removed. Due to this additional step there is a striking reduction of large errors, and the "jump" in the CDF curves for 2009–2016 is completely gone. On closer inspection of archived SVN 49 ephemeris data it is frequently the case that the status alternates from healthy to unhealthy and back again, so this case is captured efficiently by this search filter. This also put a question mark on other SVNs that do show frequent changes in health status. If we now remake the figure showing error events vs. age, we get Fig. 18. As one can see, the large errors occurring at the very start of service operation are gone, as well is the error of 152 meters of SVN 49. Remaining though are some very large errors of Block IIA (at age 21).

Fig. 19 shows the percentage of large errors happening on days with other ephemeris from same satellite sent as

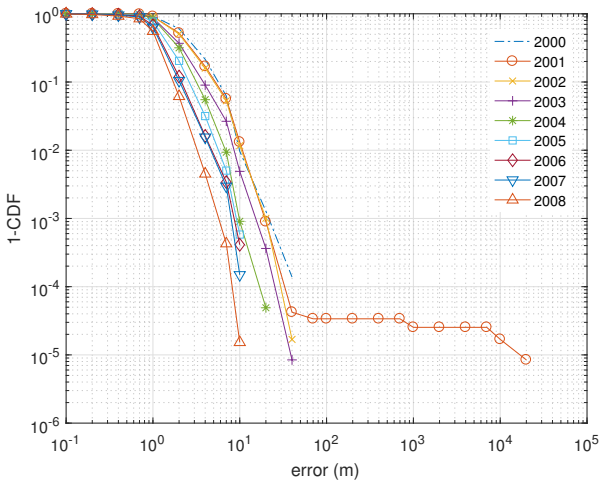


Figure 16. 2000–2008 errors of all-day healthy satellites plotted as $1-CDF$

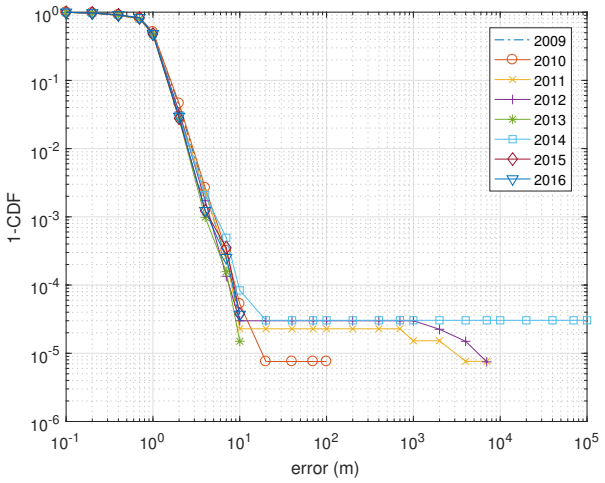


Figure 17. 2009–2016 errors of all-day healthy satellites plotted as $1-CDF$

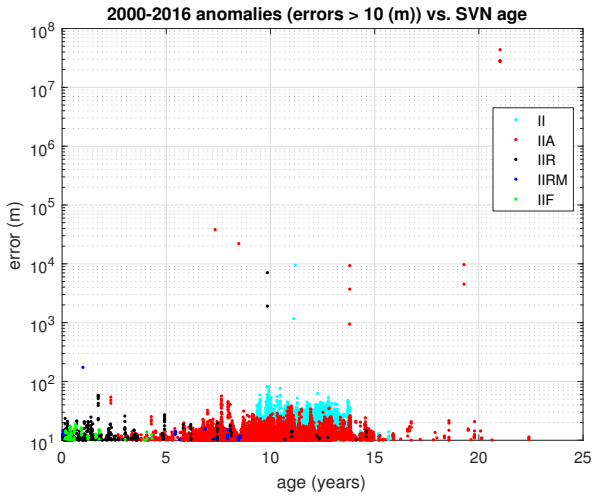


Figure 18. Large errors on pure healthy days vs. SVN age

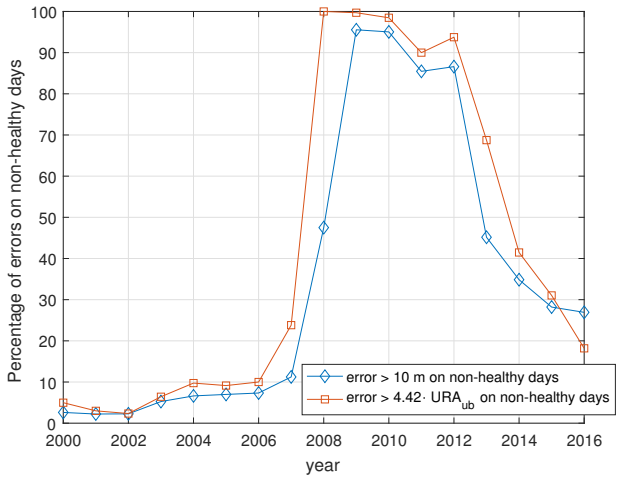


Figure 19. Large error percentage on non-healthy days including erroneously reported healthy SVN 49

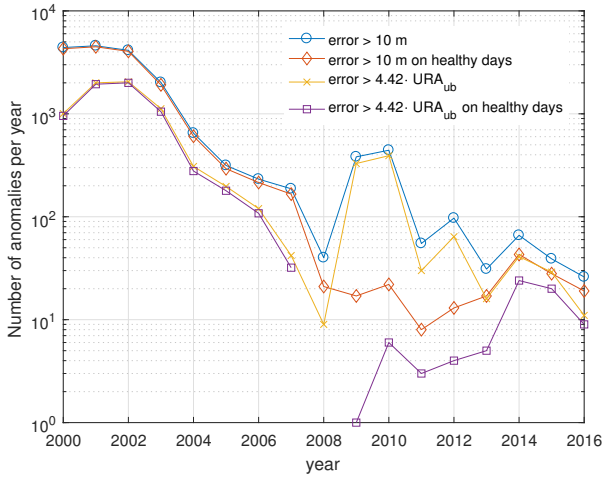


Figure 20. Number of large errors vs. year using 4 different criteria

unhealthy, using both error criteria 1 and 2. It is quite clear that such errors are almost absent in years 2000–2007, but extremely frequent in years 2008–2012. Finally, Fig. 20 shows the decay in number of large errors in the investigated years, using both error criteria. When specifically removing all SVN-49 items, we get correspondingly Fig. 21 and Fig. 22, which shows clearly the influence of improperly reported health status of the malfunctioning vehicle on the annual statistics.

Table III shows the results in numbers, where the right-most columns (starting with "Anomalies" column) are due to error criteria 2. The special SVN-49 errors are listed in separate column, and are included in the rest of the error counts and statistics, except in the two right-most columns. We note that there are two residual large errors remaining: 38151 m error in 2001, and $4.37 \cdot 10^7$ m in 2014. Further data analysis reveals that the former is due to PRN-06 in 2001 (July 13), which by that time was serviced by SVN-36, a Block II-A vehicle. SVN-36 can be seen as the next-highest peak in Fig. 23. We have investigated this period manually and find no other occurrences

Table III. CLEANSING AND LARGE ERROR ANALYSIS SUMMARIZED

| Year | Removed by "Toe offset" | Tot. Eph data | Removed by sorting | Duplicates | of which caught in triplet filter | Inconsi-stent | Cleansed | Ano-malies | SVN49 Ano-malies | Defect com-parison | Max error | Error std | Max error pure healthy days | Std pure healthy days |
|---|---|---|---|---|---|---|---|---|---|---|---|---|---|---|
| **2000** | 406 | 129038 | 0 | 9475 | 8 / 3 | 13 | 119550 | 4405 | 0 | 552 | 349 | 10 | 81.8 | 6.57 |
| **2001** | 32 | 139787 | 1229 | 15030 | 1051 / 0 | 17 | 123511 | 4581 | 0 | 418 | 38152 | 666.4 | 38151.6 | 673.60 |
| **2002** | 22 | 133264 | 692 | 11054 | 2 / 0 | 35 | 121483 | 4138 | 0 | 211 | 61 | 6 | 58.1 | 5.70 |
| **2003** | 22 | 134515 | 0 | 11598 | 0 / 0 | 6 | 122911 | 2017 | 0 | 152 | 233 | 10 | 62.3 | 5.26 |
| **2004** | 261 | 136636 | 80 | 11394 | 6 / 0 | 6 | 125156 | 649 | 0 | 73 | 189 | 10 | 34.1 | 3.90 |
| **2005** | 13 | 138689 | 0 | 11683 | 0 / 0 | 23 | 126983 | 315 | 0 | 173 | 121 | 7 | 25.0 | 3.16 |
| **2006** | 0 | 138301 | 0 | 11028 | 0 / 0 | 17 | 127256 | 232 | 0 | 171 | 484 | 31 | 26.3 | 3.52 |
| **2007** | 0 | 146613 | 0 | 11625 | 0 / 0 | 187 | 134801 | 187 | 0 | 313 | 1017 | 78 | 20.3 | 2.17 |
| **2008** | 0 | 158957 | 5612 | 17101 | 0 / 0 | 30 | 136214 | 40 | 0 | 29 | 36568981 | 7371408 | 17.6 | 1.97 |
| **2009** | 0 | 166992 | 7110 | 21018 | 0 / 0 | 140 | 138724 | 382 | 318 | 154 | 30886803 | 2207724 | 21.6 | 3.50 |
| **2010** | 0 | 172313 | 11341 | 21130 | 0 / 0 | 480 | 139362 | 443 | 375 | 221 | 52306352 | 4156932 | 173.7 | 34.16 |
| **2011** | 0 | 176450 | 16018 | 22186 | 0 / 0 | 86 | 138160 | 55 | 0 | 48 | 683208 | 116171 | 9326.7 | 3317.18 |
| **2012** | 0 | 180500 | 20315 | 22246 | 0 / 0 | 93 | 137846 | 97 | 29 | 74 | 26880 | 3119 | 9715.8 | 3250.17 |
| **2013** | 0 | 174600 | 21130 | 14997 | 0 / 0 | 59 | 138414 | 31 | 6 | 47 | 51300608 | 12525649 | 20.8 | 2.60 |
| **2014** | 0 | 165582 | 10208 | 17923 | 0 / 0 | 123 | 137328 | 66 | 6 | 156 | 43668056 | 9062848 | 43668056 | 9529036 |
| **2015** | 0 | 167725 | 10474 | 18796 | 0 / 0 | 54 | 138401 | 39 | 0 | 95 | 708627 | 113638 | 16.9 | 1.96 |
| **2016** | 0 | 162637 | 11265 | 10940 | '0 / 0' | 15 | 140417 | 26 | 0 | 8 | 19248 | 3772 | 17.5 | 2.37 |

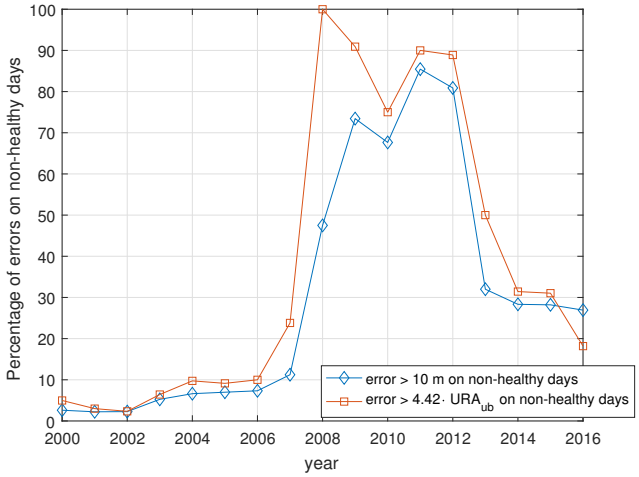


Figure 21. Large error percentage on non-healthy days excluding erroneously reported healthy SVN 49

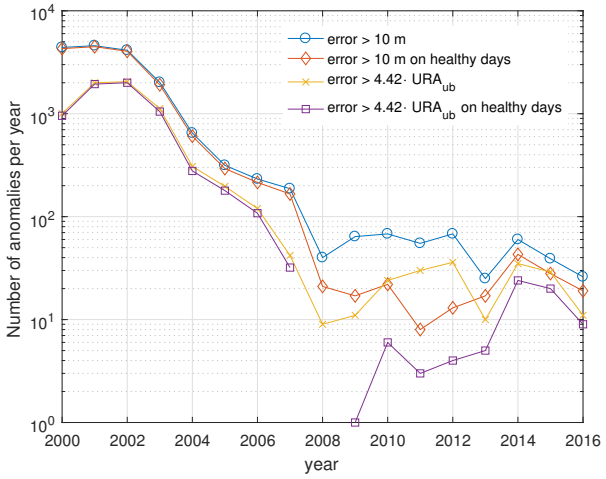


Figure 22. Number of large errors vs. year using 4 different criteria, where all SVN-49 errors are removed

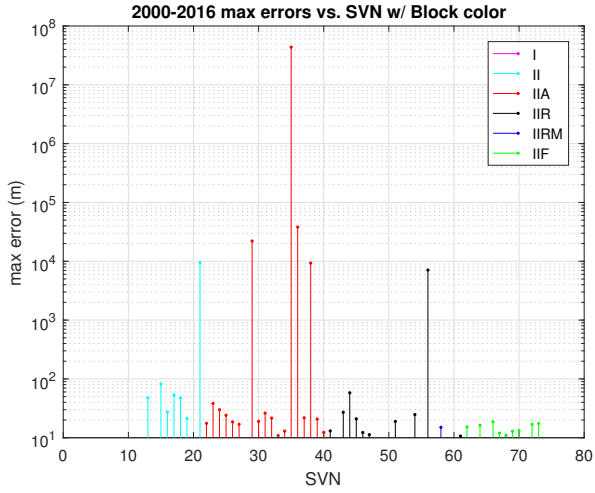


Figure 23. Maximum of large errors sizes vs. SVN, where data from partly non-healthy days are removed

of unhealthy operation at that time. The error value can be due to an error in $T_{oe}$ of 10 seconds, since vehicle velocity is approximately given by

$$v = 2\pi \cdot \frac{2.66 \cdot 10^7}{12 \cdot 3600} = 3868.8 \text{ m/s}. \quad (1)$$

The latter error of $4.37 \cdot 10^7$ m is due to PRN-03 in September 6 in 2014, which was serviced by SVN-35 of that time, starting midnight to September 5th. It can be seen as the highest peak in Fig. 23. Deeper inspection shows four large errors starting the day before, but all are logged in the ephemeris archive as healthy. However, by searching [7] again, this vehicle was out of service at that time, and not included in the broadcast almanac.

While both the large number of errors attributed to SVN-49 and the identified SVN-35 high-magnitude of error are known anomalies referenced in at least one NANU [7], the CORS data reflects representative ephemeris received and interpreted by the GPS end user terminals. Not all of the receivers take

into account almanac data due to the long period required to acquire a complete copy, which may reflect service availability correspondingly to the NANU information. This indeed raises a question regarding the Control Segment data integrity, since it can affect the GPS receivers ability to perform qualified position fix. More of the large errors detected here, but not exclusively inspected might have been flagged in other NANUs as out of services. Such inspection is left for follow-up work.

Our findings show that, referring back to the four questions investigated:

- $T_{oe}$ Are ephemeris data holding $T_{oe}$ values with two least significant digits not ending on 00 of lesser quality? Our clear finding is no, this data is in general as good as other data. See Fig.7.
- Block Are some Blocks of satellites reasonably expected to have higher error probability than others? Most of the largest errors both in numbers and magnitude stem from Block IIA, but this block is also the dominating service Block of the investigated time span. Block II shows high number of large errors, but their maximum magnitude is limited. Block IIR has very limited number of large errors, and when accounting for only pure healthy operational days, only SVN-56 has a severe single large error. The new Block IIF shows stable performance when only healthy operational days are accounted for.
- Age Will old satellite vehicles have increased probability of large errors? We do have a few very large errors of Block IIA at age about 21 years, but not a *substantial number* of the same. Many more large errors were actually found in the very start of vehicle service times as opposed to near the end of operation. Most of the latter were however found to be captured on days were at least the archived ephemeris data has frequently shifted between healthy and unhealthy.
- Healthy Is it likely that "healthy" ephemeris data will contain errors if earlier or later ephemeris close in time from same satellite have been flagged as unhealthy? Yes, we have found many occurrences of large errors on days when there also have been dispatched ephemeris data signalling unhealthy operation. It is unclear whether we can rely on the archived data in this matter, especially taking into account the many archived SVN-49 ephemeris data showing this vehicle as healthy. We also detected that it is in the years 2008–2013 that there is an especially high number of large errors on days with alternating health flag status.

## V. Conclusion

In this paper we have conducted a survey into archived GPS ephemeris data. In our cleansing algorithm, we perform sorting and inconsistency checking. Of the latter, e.g., data not complying to slowly varying $I_0$ and $\Omega_0$ are subject to removal. 10–20 % of the data was removed in the refined cleansing algorithm, producing ephemeris data set sizes inline with the expected numbers. We investigated the performance of the remainder data by calculating position errors when comparing to true satellite positions. Our findings conclude that ephemeris data having $T_{oe}$ parameter not ending on 00 is perfectly good data with an error distribution quite similar to typical data, and that ephemeris data performance has in general had a decay in the number of errors throughout the investigated period 2000–2016 (as would reasonably be expected). Nevertheless, we have found that Block IIF and IIR-M still have several large errors in their initial period of operation, though at the same time their ephemeris data is frequently alternating between healthy and unhealthy. Some large errors were attributed to the very long lived but now retired Block IIA vehicles, but no clear evidence was found that error probability was increasing with age, in turn indicating that the control segments efforts to keep these vehicles in service for an extended period yet retire them before failure was very well executed. We were surprised to find SVN-49 reporting healthy conditions in the ephemeris, since this vehicle was never put into service. Further work could including filtering of this vehicle in the cleansing part of the software, and perform a survey if any other non-serviced vehicle is still reported healthy in the ephemeris archives. In addition, continued work could include an investigation of the question if frequent shifts in health flag status also occur for ephemeris data of excellent quality, since this paper only investigated health flag shifts in "bad" data. A final labour intensive area of additional investigation could be a detailed inspection of large errors vs. NANUs to determine which of the identified large errors are in part due to either control segment error or due to receivers not properly interpreting health information on properly flagged satellites.

## Acknowledgment

The study presented in this article was partially supported by funding from the Norwegian Research Council project NORGAL (Nordic Concept for CATIII/Autoland based on GBAS), and SESAR Joint Undertaking Ref. SJU/LC/0034-CTR Project 15.3.7.

## References

[1] D. L. M. Warren and J. F. Raquet, "Broadcast vs. precise GPS ephemerides: a historical perspective," *GPS Solutions*, vol. 7, no. 3, pp. 151–156, 2003. [Online]. Available: http://dx.doi.org/10.1007/s10291-003-0065-3

[2] L. Heng, G. Gao, T. Walter, and P. Enge, *GPS ephemeris error screening and results for 2006-2009*, 2010, vol. 2, pp. 1184–1192.

[3] L. Heng, G. X. Gao, T. Walter, and P. Enge, "GPS Signal-in-Space Integrity Performance Evolution in the Last Decade," *IEEE Transactions on Aerospace and Electronic Systems*, vol. 48, no. 4, pp. 2932–2946, October 2012.

[4] (2017, Jan) GPS Satellite Outage Information. [Online]. Available: http://navigationservices.agi.com/SatelliteOutageCalendar/SOFCalendar.aspx

[5] M. J. Dunn, "IS-GPS-200G — Global Positioning Systems Directorate Systems Engineering & Integration Interface Specification," Navstar GPS Space Segment, Tech. Rep., Sep 2012.

[6] (2009, Jul) Expert Advice: Cause Identified for Pseudorange Error from New GPS Satellite SVN-49. [Online]. Available: http://gpsworld.com/tag/svn-49/

[7] (2017, Jan) GPS ALMANACS, NANUS, AND OPS ADVISORIES ARCHIVES. [Online]. Available: http://www.navcen.uscg.gov/?Do=gpsArchives&exten=txt